

Proceedings of the Korean Nuclear Society Spring Meeting  
Cheju, Korea, May 2001

## **MARS MECHANISTIC FILM-SPLITTING AND DRYOUT MODEL IN ANNULUS GEOMETRY**

Ji-Han Chun and Un-Chul Lee

Seoul National University  
San 56-1, Shinlim-dong, Gwanak, Seoul 151-742, Korea

Won-Jae Lee

Korea Atomic Energy Research Institute  
150, Dukjin-dong, Yusung, Daejeon, 305-353, Korea

### **Abstract**

Annular flow in annulus geometry is characterized as two liquid films flowing along the inner heated rod and outer unheated walls. Critical heat flux (CHF) occurs when the liquid film on the inner heated wall dries out, while there still exists the liquid film on the outer cold wall. In the MARS code, film dryout is calculated by a mechanistic model or CHF table look-up method. The mechanistic film dryout is modeled using a complex function of film flow rate, applied heat flux and entrainment/deposition rate, etc. and is determined by the hydrodynamic solution. The table look-up method interpolates the AECL-UO CHF table. However, both models were not able to distinguish the liquid films on the cold and hot surfaces in a calculation cell, that is, the cold wall effect. This resulted in over-estimation of the calculated CHF in the single-channel modeling of annulus geometry, which necessitated a new model that could consider the cold wall effect mechanistically in the single-channel modeling. In order to consider the cold wall effect, a mechanistic film splitting model has been developed for MARS implementation, in which the inner and outer liquid film fractions are solved analytically by introducing a maximum velocity plane concept in the vapor core. In addition, the droplet entrainment and deposition models and the transition criterion for the annular flow regime are improved in order to enhance code accuracy. The new MARS version has been assessed using the KAERI annulus CHF tests and the results shows enhanced agreement with the experimental data.

### **1. Introduction**

CHF is defined as a discontinuous reduction of the local heat transfer coefficient, which results from the replacement of liquid by vapor on a heated surface. This phenomenon is of major

importance in nuclear reactor safety, since fuel failure due to a rapid heat-up by CHF may lead to the release of radioactive materials into environment. CHF phenomenon is classified into two kinds of mechanisms. One is called as the Departure of Nucleate Boiling (DNB), in which the vapor blanket covering the heated surface deteriorates the heat transfer rate. Heat transfer regime transits from subcooled or saturated nucleate boiling to film boiling. DNB has been the major safety concern of pressurized water reactor (PWR) transients and it occurs when the surface heat flux is relatively high and the void quality is low. The other mechanism is annular film dryout, in which a continuous liquid film on the heated surface is dried out by droplet entrainment and the evaporation. The dryout mechanism has been the main safety concern of not only the boiling water reactor transients. Dryout occurs in an annular flow regime when the void quality is relatively high.

Most of the thermal-hydraulic transient codes for PWRs use a CHF look-up table method or experimental CHF correlations specific to fuel design. Since DNB has been the major safety issue of PWR safety, there are a lot of experimental databases available for DNB, however, there are few experimental and analytical databases for dryout. It is quite recent that the importance of dryout models gets highlighted for PWR analysis. With the introduction of a best-estimate analysis method to the design-basis and the beyond design-basis accident analysis, the dryout phenomena in the core and the steam generator became emphasized for the realistic prediction of transient system response. In this context, KAERI performed dryout tests in an annulus geometry at high quality and low mass flux (Chun et al., 1998). KAERI will perform further tests for a 3x3 fuel bundle in the near future.

KAERI developed the MARS code for the multi-dimensional system thermal hydraulic analysis of light water reactor transients as well as nuclear and non-nuclear facilities (Lee et al., 1999). MARS consists of a one-dimensional (1-D) module for 1-D modeling of the reactor coolant system and a three-dimensional module for multi-dimensional modeling of the reactor vessel or steam generator secondary side. The three-dimensional module of the code employs 3-field 2-fluid equations (liquid phase, gas phase and droplet phase), and uses a mechanistic model for liquid film dryout. MARS predicted reasonable results for a pipe geometry, but the results were overestimated for an annulus geometry because the cold wall effect could not be taken into account in the code (Chun et al., 1999). In annular flow, liquid films exist on the unheated wall as well as the heated wall. The dryout on the heated wall occurs when the liquid film on the inner heated wall dries out, whereas there is still a considerable liquid film on the outer unheated wall. This is called the cold wall effect, however, MARS was not able to consider two films in a calculation cell. Therefore, it became necessary to develop a new mechanistic model that can discriminate the inner and outer liquid film fractions in annular flow. In this study, a mechanistic film splitting model (Levy et al., 1980), that solves the splitting of liquid film by introducing a maximum velocity condition in the vapor core, was developed for application to MARS. A pilot code for this model was then developed, which is used to generate a liquid film look-up table for MARS implementation. In addition, droplet entrainment and deposition models and the transition criterion for an annular flow regime were improved in order to enhance MARS accuracy. In order to verify and validate the new models, KAERI annulus CHF tests were assessed.

## **2. MARS Dryout Model**

Since the core or the steam generator secondary side is modeled using the 3-D module of MARS, thermal-hydraulic models of the 3-D module relevant to the dryout are discussed in this section.

## 2.1 Governing Equations

The 3-D module of MARS (Lee et al., 1999) employs a two-fluid, three-field representation of two-phase flow. Each field is treated three dimensionally with a compressible flow condition. Continuous vapor, continuous liquid and entrained liquid droplets are treated as independent fields with interfacial interaction. The conservation equations for each field are solved using a semi-implicit, finite-difference numerical scheme on an Eulerian mesh. Another constitutive equation and flow regime map are included. One should note that MARS employs special models for droplet entrainment and deposition that are used for the transport of the droplet interfacial area.

### Mass conservation equation

$$\frac{\partial}{\partial t}(\mathbf{a}_k \mathbf{r}_k) + \nabla \cdot (\mathbf{a}_k \mathbf{r}_k \underline{U}_k) = \Gamma_k^m$$

### Momentum conservation equation

$$\frac{\partial}{\partial t}(\mathbf{a}_k \mathbf{r}_k \underline{U}_k) + \nabla \cdot (\mathbf{a}_k \mathbf{r}_k \underline{U}_k \underline{U}_k) = -\mathbf{a}_k \nabla P + \mathbf{a}_k \mathbf{r}_k g + \nabla \cdot [\mathbf{a}_k (\underline{\mathbf{t}}_k + \underline{\mathbf{T}}_k^T)] + \underline{M}_k^\Gamma + \underline{M}_k^d$$

### Energy conservation equation

$$\frac{\partial}{\partial t}(\mathbf{a}_k \mathbf{r}_k h_k) + \nabla \cdot (\mathbf{a}_k \mathbf{r}_k h_k \underline{U}_k) = -\nabla \cdot [\mathbf{a}_k (\underline{Q}_k + \underline{q}_k^T)] + \Gamma_k h_k^i + q_{T_k}^m + \mathbf{a}_k \frac{\partial P}{\partial t}$$

## 2.2 Flow Regime Map

A flow regime map of the 3-D module is based on the vertical one-dimensional flow and consists of 4 regions for bubbly, slug, churn-turbulent and annular flow regimes. The transition criteria are given as:

- ◆ Bubbly flow: from 0 to 0.2
- ◆ Slug flow: from 0.2 to 0.5
- ◆ Churn-turbulent flow: from 0.5 to  $\alpha_{\text{crit}}$
- ◆ Annular flow: from  $\alpha_{\text{crit}}$  to 1.0

$\alpha_{\text{crit}}$  is a critical void fraction, the minimum of this value is 0.8.

$$\mathbf{a}_{\text{crit}} = 1.0 - 4.0 C_1 \mathbf{s} / (\mathbf{r}_v |\underline{U}_v|^2 D_H)$$

## 2.3 Mechanistic Film Dryout Model

The heat transfer regime map specific to mechanistic film dryout is shown in Figure 1. Transition to the post-Dryout regimes is modeled to occur when the continuous liquid fraction is less than 0.01. The Zuber CHF model (Thurgood et al., 1983) is modified to generate a new CHF for application to film dryout as:

$$q''_{CHF} = \frac{P}{24} h_{fg} r_g^{0.5} [g_c g_s (r_f - r_g)]^{0.25} \times \max[0.2, 200(a_f - 0.005)]$$

To calculate CHF surface temperature ( $T_{CHF}$ ), the following equation is used.

$$q''_{CHEN}(T_{CHF}) = q''_{CHF}$$

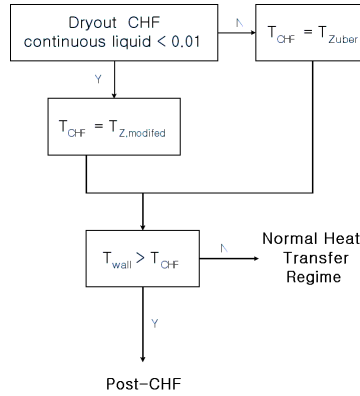


Figure 1 Mechanistic Dryout Heat Transfer Regime Map

#### 2.4 AECL-UO CHF Look-up Table Model

The 1986 AECL-UO CHF lookup table (INEEL, 1998) is used as an option in MARS. This table is made from tube data normalized to a tube inside diameter of 0.008 m, but has correction factors that are applied to allow its use in other sized tubes or in rod bundles. In addition, it considers both forward and reverse flow, axial power shape, and the effect of boundary layer changes at both the bundle inlet and behind grid spacers. The lookup table was formulated from 15,000 data points to make a three-dimensional table with 4,410 points in a three-dimensional array covering 15 pressures from 0.1 to 20.0 Mpa, 14 values of mass flux from 0.0 to 7,500.0 kg/m<sup>2</sup>s, and 21 equilibrium qualities from -0.5 to 1.0. After finding the CHF from the table, multiplying factors are used to modify the table value.

For the CHF prediction in an annulus geometry, the correction factors suggested by Doerffer, et al (1994) were implemented in MARS, where the effect of quality, gap size and pressure are taken into account as:

$$CHF_{An} = CHF_{D=8} k_x k_d k_p$$

where,  $\kappa_x$ ,  $\kappa_d$  and  $\kappa_p$  are correction factors for quality, gap size and pressure.

### 3. Improvement of MARS Dryout Model

#### 3.1 Mechanistic Film-Splitting Model of Annular Flow in an Annulus Geometry

Annular flow in an annulus geometry is characterized as two liquid films flowing along the inner heated rod and outer unheated wall, whereas gas together with entrained droplets flows through the gas core. However, the existence of two films in a calculation cell cannot be distinguished in the MARS code. This results in the overestimation of dryout in the previous assessments (Chun, et. al, 1999). To overcome such deficiency, a new mechanistic film-splitting model was developed, in which the continuous liquid mass flux calculated by MARS is subdivided into two film mass fluxes, the liquid mass flux at the outer unheated wall and that at the inner heated wall.

The MARS hydrodynamics calculate the absolute mass flows for gas, continuous liquid and entrained droplets and the liquid velocities, which would be used at best in the MARS film-splitting model. Only the continuous liquid mass phase needs to be split in MARS, whereas the mass flows of gas and the entrained droplets are the input for the MARS model.

In order to develop new film splitting model for the MARS code, the assumptions are introduced as follows. First, annular flow consists of two continuous film regions and a vapor core region in which continuous vapor and liquid droplets are uniformly mixed. The vapor core region is divided into two regions (outside and inside) according to the location of the maximum velocity plane as shown in Figure 2. (Levy et al., 1980) The velocity profiles in the vapor core regions are then assumed in the form of a single-phase universal profile from the law of the wall. The velocities of the liquid films are uniform respectively.

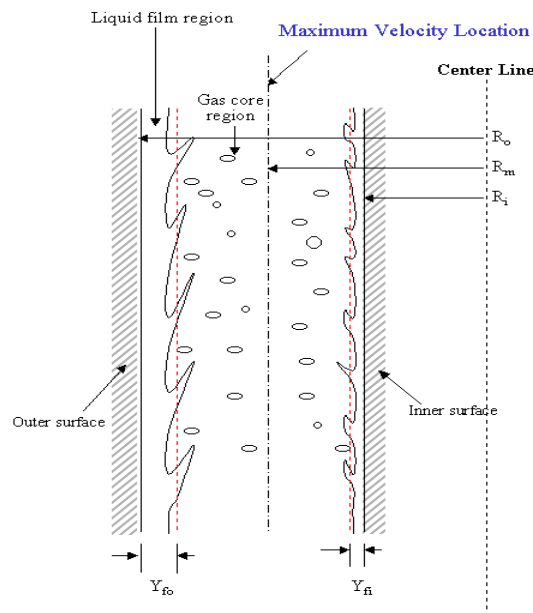


Figure 2 Schematics of the Film-Splitting Model

Using the above assumptions, we can get the velocity profiles as:

### Core vapor regions

$$u_{co}^+ = \frac{1}{k_o} \ln \left( \frac{y}{Y_{fo}} \right) + 5.5 \quad \text{outer side}$$

$$u_{ci}^+ = A_i \ln \left( \frac{y}{Y_{fi}} \right) + B_i \quad \text{inner side,}$$

The coefficients  $A_i$  and  $B_i$  of inner side velocity profiles are proposed by many researchers. Ballou et al. produced this value by fitting several experimental data banks. In this study, the Ballou' correlation are used because of the wide application range. For the range of this correlation is given as  $R_i/R_o > 0.1$ .

$$A_i = 2.7 \left( \frac{R_i}{R_o} \right)^{0.353}, \quad B_i = 3.6 \left( \frac{R_i}{R_o} \right)^{-0.439}$$

The universal velocity  $u^+$  is defined from the following equation.

$$u^+ = u / \sqrt{\frac{t_R}{r}}$$

and, the mixing length constant  $k_o$  of 0.4 is commonly used.

Calculation procedures of the new film-splitting model are as follows:

1. Guess the location of the maximum velocity location ( $R_m$ ).
2. Guess the outside film thickness ( $Y_{fo}$ ).
3. Calculate the liquid fraction of outside film as:

$$a_{fo} = \frac{R_o^2 - (R_o - Y_{fo})^2}{R_o^2 - R_i^2}$$

4. Guess the inside film thickness ( $Y_{fi}$ ).
5. Calculate the ratio of the outside interfacial shear stress to that of inside. This ratio is calculated from the pressure drop in each side.

$$\frac{t_{io}}{t_{ii}} = \frac{R_i + Y_{fi}}{R_o - Y_{fo}} \frac{(R_o - Y_{fo})^2 - R_m^2}{R_m^2 - (R_i + Y_{fi})^2}$$

6. The liquid fraction of inside film.

$$a_{fi} = \frac{(R_i + Y_{fi})^2 - R_i^2}{R_o^2 - R_i^2}$$

7. Find  $Y_{fi}$  that satisfies the continuity of gas core velocity at  $R_m$ .

$$\sqrt{\frac{t_{io}}{t_{ii}}} \left[ \frac{1}{k_o} \ln \left( \frac{R_o - R_m}{Y_{fo}} \right) + 5.5 \right] = A_i \ln \left( \frac{R_m - R_i}{Y_{fi}} \right) + B_i$$

8. Determine  $Y_{fo}$  that satisfies the condition which the sum of outside and inside liquid fraction is equal to that calculated from MARS.

$$\mathbf{a}_{fo} + \mathbf{a}_{fi} = \mathbf{a}_{f,MARS}$$

9. To determine  $R_m$ , repeat from step 1 to step 8 until the continuity of the eddy diffusivity at  $R_m$  is satisfied. The inner and outer liquid film thicknesses and liquid fractions satisfying this condition are then determined.

$$k_o(R_o - R_m) \sqrt{\frac{\mathbf{t}_{i_o}}{\mathbf{r}}} = \frac{1}{A_i} (R_m - R_i) \sqrt{\frac{\mathbf{t}_{i_o}}{\mathbf{r}}}$$

The ratio of outside wall shear stress to that at inside wall is obtained as:

$$\frac{\mathbf{t}_{R_o}}{\mathbf{t}_{R_i}} = \frac{R_i}{R_o} \frac{R_o^2 - R_m^2}{R_m^2 - R_i^2}$$

The following relationship is obtained from the definition of wall shear stress. Here, the Blasius correlation is used in order to determine the wall friction factor at both sides.

$$\frac{\mathbf{t}_{R_o}}{\mathbf{t}_{R_i}} = \frac{f_{fo} \mathbf{r}_L u_{fo}^2 / 2}{f_{fi} \mathbf{r}_L u_{fi}^2 / 2} = \frac{\text{Re}_{fo}^{-0.25} u_{fo}^2}{\text{Re}_{fi}^{-0.25} u_{fi}^2} = \frac{\mathbf{a}_{fo}^{-0.25} u_{fo}^{1.75}}{\mathbf{a}_{fi}^{-0.25} u_{fi}^{1.75}}$$

From above equation, the ratio of outer film velocity to inside film velocity becomes.

$$\frac{u_{fo}}{u_{fi}} = \left( \frac{\mathbf{a}_{fo}}{\mathbf{a}_{fi}} \right)^{1/7} \left( \frac{\mathbf{t}_{R_o}}{\mathbf{t}_{R_i}} \right)^{1/1.75}$$

Finally, the ratio of each side liquid mass fluxes to total liquid mass flux is calculated using the liquid fractions in each side and liquid film velocity ratio.

$$\frac{G_{fo}}{G_{fi}} = \left( \frac{\mathbf{a}_{fo}}{\mathbf{a}_{fi}} \right) \left( \frac{u_{fo}}{u_{fi}} \right)$$

$$\frac{G_{fo}}{G_f} = \frac{G_{fo} / G_{fi}}{1 + G_{fo} / G_{fi}}$$

### 3.2 Assessment of Mechanistic Film-Splitting Model

Based on the new film-splitting model, a pilot code has been developed and examined for accuracy. In order to examine the effectiveness of the new film-splitting model, Wurtz' experimental data (Wurtz et al., 1978) has been assessed. Test 17/26L was selected for the assessment, which are the steam-water annular flow tests in annulus geometry in adiabatic conditions. The annulus geometry has an outer diameter of 0.026 m and inner rod of 0.017 m. The pressure ranges from 30 to 90 bars and the quality ranges from 20 to 60 %. In the tests, the flow rate and thickness of the liquid films were measured by varying the inlet mass flow and the exit quality.

From the pilot code assessment, it was found that the outside film flows were underestimated slightly and the inner flow rates were overestimated as shown in Figure 3. Since the pilot code simply splits the continuous liquid flow into the inner and outer flow, even the slight underestimation of the outer flow may result in a larger deviation of the inner flow.

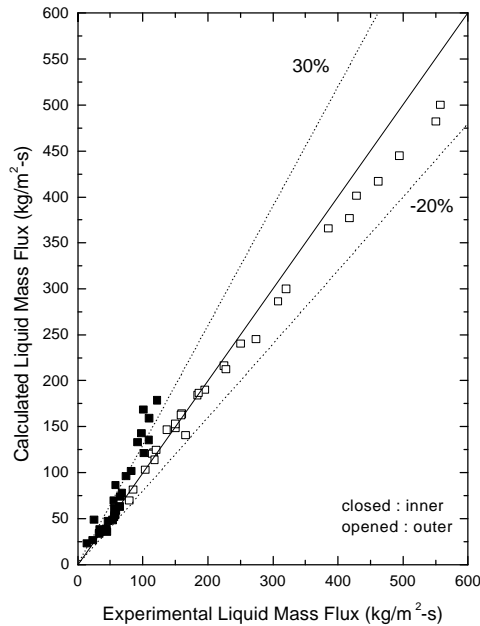


Figure 3 Comparison of Outer and Inner Liquid Mass Fluxes

### 3.3 Improvement of MARS Dryout Model

#### 3.3.1 Implementation of the Mechanistic Film-Splitting Model

There are two methods for implementing the film-splitting model into MARS, that is, direct implementation and a table search. Since direct implementation might result in an increase of calculation time due to the iteration to find the solution, it was decided to adopt the table search method.

The film-splitting table was generated using the pilot code to cover a variety of ranges of ratio of inner radius to outer radius and continuous liquid fraction. The applicable ranges of the table are:

- ◆  $R_i/R_o$  1.0 - 10
- ◆ Continuous liquid fraction 0.0001 – 0.3

The new film-splitting model was implemented in MARS in the procedures described in the following. The basic concept of implementation and the new heat transfer regime map for dryout is given in Figure 4.

- 1) The model is turned on when the flow regime reaches annular flow
- 2) Add the vapor generation rate to the total liquid mass flow calculated by MARS, that is, obtain

- the total liquid mass flow before vapor generation in the liquid film by heat transfer
- 3) Search the film-splitting table in order to obtain inner and outer liquid film flow using the search variables.
  - 4) Extract the vapor generation rate from the inner liquid film flow, then the final inner liquid film flow is obtained
  - 5) If the compensated inner liquid film flow is less than the dryout criteria, the post-CHF heat transfer regime is invoked

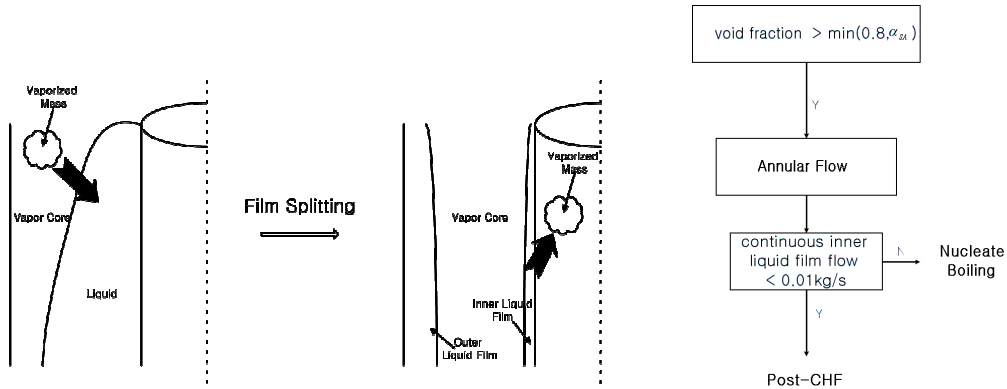


Figure 4 Dryout Model Implementation

### 3.3.2 Improvement of the Droplet Entrainment/Deposition Model

The entrainment and deposition of liquid droplets in annular flow affects the amount of continuous liquid film and consequently the inner liquid film flow. MARS employs Wurtz and Cousins models (Thurgood et al., 1983) as the entrainment and deposition models. It was found that the Wurtz model estimates the entrainment rate well at high quality (above 0.6), but it under-estimates the entrainment rate at low quality (Ha et al., 1998). To improve this, the modified Sugawara model (Ezzidi et al., 1993) was implemented in MARS.

The modified Sugawara model introduced some factors to the Wurtz model for better agreement for wide ranges of experimental data. Those were the pressure effect terms represented by the density ratio and the flow factor represented by the ratio of Reynolds number (Ezzidi et al., 1993). The final expressions of entrainment and deposition rate are:

$$m_E = 0.219 \left( \frac{t_l \Delta h}{s} \right) \left( \frac{u_v m_l}{s g} \right) \left( \frac{r_l}{r_v} \right)^{0.4} \left( \frac{Re_l}{Re_{vl}} \right)^{0.235}$$

$$m_{DE} = 9.0 \times 10^{-3} \left( \frac{C}{r_v} \right)^{-0.5} Re^{-0.2} Sc^{-2/3} u_v C$$

### 3.3.3 Improvement of Annular Flow Transition Criteria

The transition to annular flow regime is also of importance in correctly estimating the amount of droplet entrainment in MARS. Since the 3D module of MARS had been developed mainly for

reflood physics, the annular flow transition criterion is not suitable for a high pressure response, that is, it was found that the criterion over-estimates the critical void fraction at high pressure. To overcome such deficiency, the annular flow transition criterion is improved by introducing the RELAP5 model (INEEL, 1998) that was verified as applicable to the high pressure range as:

$$\mathbf{a}_{SA} = \max \left[ 0.5, \min \left( \mathbf{a}_{crit}^f, \mathbf{a}_{crit}^e, 0.9 \right) \right]$$

where,  $\mathbf{a}_{crit}^f = \frac{1}{v_g} \left[ \frac{gD (r_f - r_g)}{r_g} \right]^{1/2}$  and  $\mathbf{a}_{crit}^e = \frac{3.2}{v_g} \left[ \frac{gs (r_f - r_g)}{r_g^2} \right]^{1/4}$

## 4. MARS Dryout Model Assessment

### 4.1 Test Section Modeling

In order to validate the new film-splitting dryout model of MARS, the KAERI annulus CHF tests were assessed. The test was performed in the RCS loop facility (Reactor Coolant System thermal hydraulics loop facility) of KAERI. The inner diameter of the annulus test section is 19.4mm and the outer diameter of the inner heated rod is 9.54mm with a heating length of 1842mm. The steady state and transient CHF tests were performed for uniform and cosine power profiles. The ranges of test conditions are (Chun et al., 1998):

- ◆ Operating pressure                      0.5 – 16 Mpa
- ◆ Test section water flow rate            0.03 – 3 kg/s
- ◆ Max. water temperature                620 K
- ◆ Available heating power of test section 500kW
- ◆ Inlet Subcooling :                        80 - 350 kJ/kg

The test section is modeled as a single flow channel as shown in Figure 5. In order to reflect the effect of the power profile, test section is axially divided into 10 nodes for the uniform power tests and the cosine power tests having non-equal length. The inlet and outlet parts of the test section are model as boundary volumes and junctions.

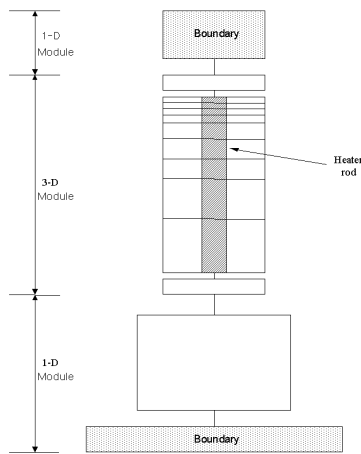


Figure 5 Test section modeling

#### 4.2 Original MARS Dryout Model Assessment

Figure 6 and 7 show the MARS assessment results in the previous study (Chun et al., 1999). The original mechanistic dryout model and the CHF look-up model are assessed respectively. As shown in these figures, the MARS mechanistic model and the look-up table model without the annulus correction factors highly over-estimated the CHF. With the annulus correction factors, the calculation became closer to the test data, but still consistently over-estimated the data. It was concluded from the previous study that the major reason of the over-estimation is due to neglecting the cold wall effect. This necessitated the development of a new model that can mechanically estimate the cold wall effect through the splitting of a continuous liquid film on the outer and inner walls.

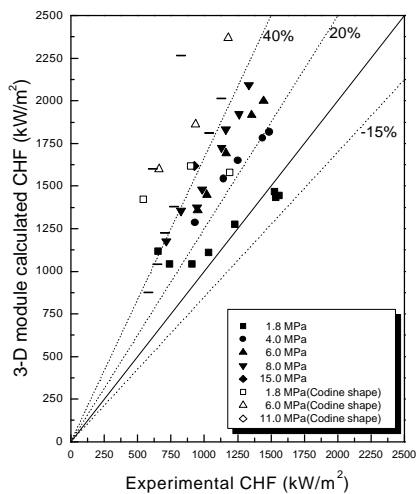


Figure 6 Original Mechanistic Model

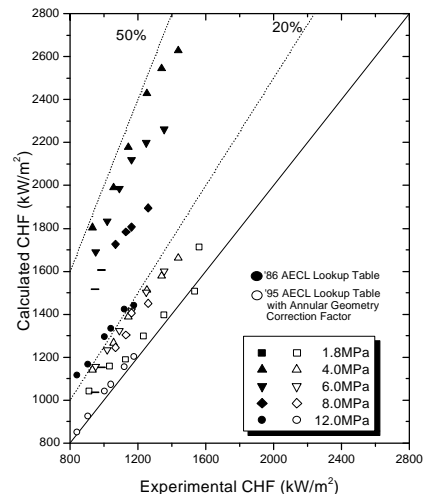


Figure 7 CHF Lookup Table Model

### 4.3 Improved MARS Dryout Model Assessment

The new mechanistic film-splitting model of MARS has been assessed. A comparison with the steady state tests is shown in Figure 8. With the new model, the predictability of MARS is remarkably enhanced in comparison with the previous assessments such that most of the calculation results for the steady state uniform and cosine power tests are evenly within 20% deviation. Figure 9 represents the assessment results to the transient CHF tests. It also shows that the most of deviations are within 20%.

From the assessments, it can be concluded that the new film-splitting model needs more improvement for better accuracy.

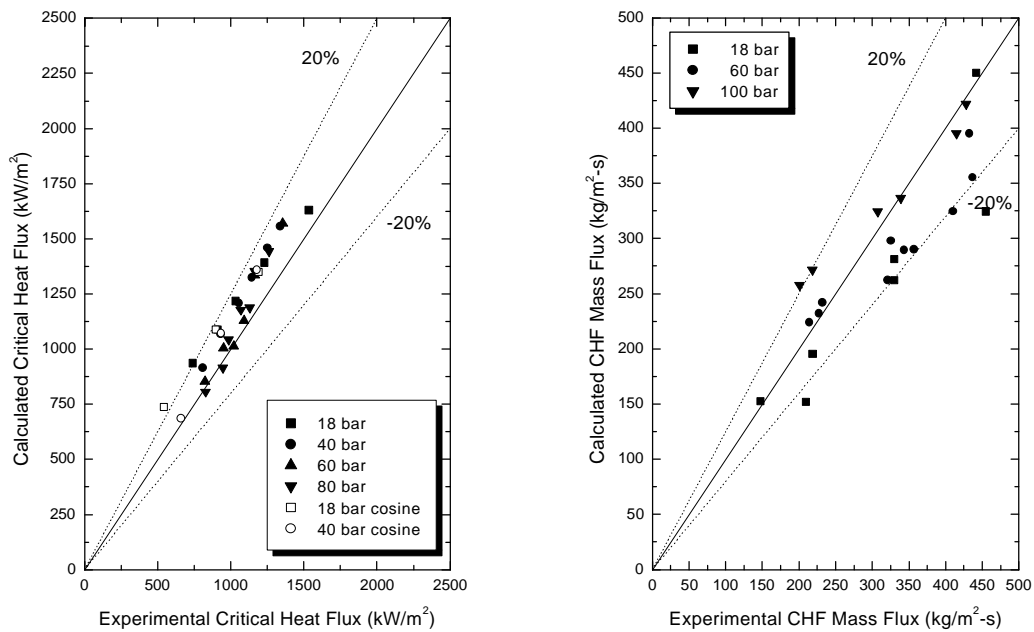


Figure 8 Film-Splitting Model – Steady Test Figure 9 Film-Splitting Model – Transient Test

## 5. Conclusions and Future Works

The MARS dryout model has been improved by incorporating the new mechanistic film-splitting model for annular flow in annulus geometry, the improved droplet entrainment and deposition models and the improved transition criterion for annular flow. Mechanistic film splitting in annulus geometry is modeled in the code by using a film-splitting look-up table. The look-up table was generated by a pilot code that calculated the mechanistic film-splitting in various flow conditions. Dryout is defined in the MARS when the film on the heated wall is dried out. The new MARS model was assessed using the KAERI annulus CHF tests. The assessment results show that the accuracy of the new model is remarkably enhanced compared to the previous assessment results. For future work, we will extend the model to other flow geometries and

continue the model assessment using experimental experiments having various flow geometries and flow conditions.

## Nomenclature

U,u : velocity  
P : pressure  
g : acceleration of gravity  
T : turbulent stress tensor  
 $M^T$  : supply of momentum due to mass transfer  
 $M^d$  : drag force  
h : enthalpy  
 $h^i$  : surface enthalpy  
Q : conduction vector  
 $q^T$  : turbulent heat flux  
 $q''$  : heat flux  
 $u^+$  : non-dimensional velocity  
k : turbulent mixing length constant  
G : mass flux

### Greek

$\alpha$  : void fraction  
 $\rho$  : density  
 $\Gamma$  : mass transfer rate  
 $\sigma$  : surface tension  
 $\beta$  : density function exponent  
 $\tau$  : viscous stress tensor  
 $\kappa$  : annulus correction factor  
 $\delta$  : gap size

### Subscript

k : each phase  
v,g : vapor  
l,f : liquid  
crit : critical  
vl : relative quantity between vapor and liquid  
o : outer wall  
i : inner wall  
m : maximum velocity location  
c : core region  
w : transition layer region  
MARS : quantity from MARS  
E : entrainment  
DE : deposition

SA : transition from slug to annular flow  
CHF,c : critical heat flux  
CHEN : Chen correlation

### **Acknowledgement**

This study has been performed under the Nuclear R&D of MOST (Ministry of Science and Technology)

### **Reference**

- Chun, S. Y., et al. (1998). "Effect of Pressure on Critical Heat Flux in Vertical Annulus Flow Channel under Low Flow Condition", Proceeding of NTHAS98, 342-347
- Chun, J. H., et al. (1999). "Assessment of MARS 1.4 Dryout Model Using KAERI Annulus CHF Test", Proceeding of KSME Conference, 607-613
- Doerffer, S., et al. (1994). "A Comparison of Critical Heat Flux in Tubes and Annuli", Nuclear Engineering and Design, 149, 167-175
- Ezzidi, A., et al. (1993). "Improvement of COBRA-TF Code Models for Liquid Entrainment in Film-Mist Flow", JAERI-M 93-133
- Ha, K. S., et al. (1998). "Improvement of Liquid Droplet Entrainment Model in the COBRA-TF Code", Journal of the Korean Nuclear Society, 30(3), 181-193
- INEEL (1998). "RELAP5/MOD3 Code Manual Volume IV: Models and Correlations", USNRC, NUREG/CR-5535
- Lee, W. J., et al. (1999). "Improved Features of MARS 1.4 and Verification", KEARI/TR-1386-99
- Levy, S., et al. (1980). "Analysis of Annular Liquid-Gas Flow with Entrainment Cocurrent vertical Flow in an Annulus", EPRI report, NP-1563
- Thurgood, M. J., et al. (1983). "COBRA/TRAC – A Thermal-Hydraulics Code for Transient Analysis of Nuclear Reactor Vessels and Primary Coolant Systems: Equations and Constitutive Models", NUREG/CR-3046
- Wurtz, J., et al. (1978). "An Experimental and Theoretical Investigation of Annular Steam-Water Flow in Tubes and Annuli at 30 to 90 bar", Riso report, No. 372